UNCERTAINTY ANALYSIS IN SEISMIC EVENT LOCATION

William Rodi and M. Nafi Toksöz

Massachusetts Institute of Technology

Sponsored by Defense Threat Reduction Agency

Contract No. DTRA01-00-C-0102

ABSTRACT

Uncertainty in event locations derived from seismic data is caused by errors in the arrival times of picked phases, misidentification of seismic phases, and errors in the travel-time model used in the location process. The event mislocation induced by these error sources is affected by the number and spatial distribution of stations that record an event. This project is developing a statistical framework and computational techniques for accurately analyzing event location uncertainty. Our statistical approach is based on a maximum-likelihood framework, which defines an optimal location estimate to be that maximizing a likelihood function, and derives confidence regions in terms of hypothesis tests applied to likelihood ratios. An appropriate likelihood function is prescribed in terms of a probabilistic model of the various types of errors in seismic data. With appropriate computational tools, it is possible to implement a general class of error models that allow for non-Gaussian distributions, spatially correlated errors in travel-time tables, and other complexities that conventional location algorithms do not handle. Additionally, the assumption of local linearity of the forward problem (travel-time vs. location) can be avoided. We are developing such computational tools based on grid-search and Monte-Carlo simulation techniques. We have implemented our statistical formulation in a general event location algorithm that finds optimal location estimates from arrival time, slowness and azimuth measurements for regional and teleseismic phases, and computes the non-elliptical confidence regions which follow from a general error model and nonlinear analysis. We have used the algorithm to study the effects of nonlinearity and non-Gaussian error assumptions on the confidence regions of sparsely recorded events, applying it to regional arrival data from the 1991 Racha earthquake sequence, data from local and national networks in Turkey, and from the Reviewed Event Bulletin of the International Data Centre. Our present efforts focus on developing a realistic and practical formulation of the errors in the travel-time tables that are used in locating events ("modeling errors"). We are basing our formulation on empirical methods for estimating travel-time corrections from multiple-event data sets, with the goal of deriving location confidence regions that properly reflect the results of network calibration studies.

KEY WORDS: seismic event location, location uncertainty, confidence regions

OBJECTIVE

The objective of this work is to develop a methodology for seismic event location that provides reliable estimates of location uncertainty that can be used in nuclear event monitoring. Conventional methods for inferring confidence regions on event locations employ assumptions that may not be valid in the case of small, sparsely recorded events. These assumptions include local linearity of the travel time vs. hypocenter forward model and the treatment of errors in arrival time picks and travel-time models as uncorrelated, Gaussian random variables. The linear approximations used in computing standard, elliptically shaped confidence regions are only appropriate when the "true" confidence region for an event is small compared to the distances to stations, and does not include large velocity variations. Gaussian error models do not capture the observational difficulties of correctly identifying and picking low signal-to-noise arrivals (Jeffreys, 1932). Further, they are an ad hoc representation of what is often a larger source of error: the errors in the travel-time tables used in locating an event. We are attempting to address these difficulties by developing a general theoretical framework and computational tools for uncertainty analysis in seismic event location.

RESEARCH ACCOMPLISHED

Theoretical Formulation

Our approach to seismic event location is based on a maximum-likelihood formulation. We define an optimal location for a seismic event to be that which maximizes a likelihood function, constructed on the basis of an assumed statistical model of errors in the seismic data used in locating the event. Confidence regions are defined in terms of hypothesis tests using likelihood ratios as the test statistics. We have formulated and implemented this approach for three types of seismic data used in nuclear monitoring: arrival times, azimuths and slownesses. To simplify the discussion here, we consider only arrival times.

The hypocentral parameters of a seismic event are an origin time t and location $\mathbf{x} \equiv (\theta, \phi, z)$, where θ is latitude, ϕ is longitude and z is depth. Let $\mathbf{d} = (d_1, d_2 \ldots, d_n)$ be an n-dimensional vector of arrival times picked from various seismic phases at a seismic network. The event location problem may be expressed as

$$d_i = t + T_i(\mathbf{x}) + c_i + e_i, \quad i = 1, \ldots, n. \tag{1}$$

T_i is a travel-time function for the ith datum, which in our algorithms is evaluated by interpolating a travel-time table, sampling travel-time as a function of epicentral distance and event depth (for a 1-D earth model) or as a function of $\mathbf{x}$ (for a 3-D earth model). The term e_i denotes the observational, or picking, error in d_i. The term c_i can be interpreted in two ways. First, it is a correction to $T_i(\mathbf{x})$, accounting for the difference between the travel-time function and the true travel times in the Earth. However, if c_i is not known, it can be considered an additional source of error in d_i, and from this view it is sometimes referred to as a "modeling error." In our formulation, we assume that any known corrections have been included in T_i, leaving c_i as an unknown error. The uncertainty analysis for the event hypocenter $\mathbf{x}$ must account for the combined error, $c_i + e_i$.

Our current algorithms assume that the picking errors are statistically independent and, following Billings et al (1994), that each is distributed with an exponential power distribution, whose probability density function (p.d.f.) is given by

$$f(e_i) = \frac{1}{K(p)\sigma_i} \exp\left\{ -\frac{1}{p} \left| \frac{e_i}{\sigma_i} \right|^p \right\} \tag{2}$$

where the scale parameter σ_i is a standard error, $K(p) = 2p^{1/p}\Gamma(1+1/p)$, and Γ is the gamma function. When $p = 2$, then e_i is normally distributed with a mean of zero and variance of $(\sigma_i)^2$. When $p = 1$, it is exponentially distributed. We assume that the standard errors are known in a relative sense and write

$$\sigma_i = \sigma \nu_i \tag{3}$$

where the ν_i are known but the universal scale parameter, σ, is not. For the moment, we will ignore the modeling errors and assume $c_i = 0$.

The joint p.d.f. of the n data is the product of the error p.d.f.'s. Considered as a function of the unknown parameters ($\mathbf{x}$, t, and σ) this joint p.d.f. is the likelihood function we seek to maximize. Denoting it as $L(\mathbf{x}, t, \sigma, \mathbf{d})$ our assumptions imply

$$-\log L(\mathbf{x}, t, \sigma; d) = \sum_{i=1}^{n} \log \nu_i + n \log K(p) + n \log \sigma + \frac{1}{p\sigma^p} \sum_{i=1}^{n} \left| d_i - t - T_i(\mathbf{x}) \right|^p \Big/ (\nu_i)^p . \tag{4}$$

We denote the maximum-likelihood estimates of the unknowns as $\mathbf{x}_{m1}$, t_{m1}, and σ_{m1}. The maximization may be subjected to prior constraints on the parameters. For the applications here the constraints of interest are

$$0 \le z \le z^{\max} \tag{5}$$

$$\sigma^{\min} \le z \le \sigma^{\max}. \tag{6}$$

From the point of view of finding **x** and *t*, maximizing *L* is equivalent to minimizing the last term of equation (4), which is just a norm of data residuals. For example, with $p = 2$ the problem reduces to nonlinear least squares. However, with error models more general than we consider here, allowing for example asymmetric or multi-modal error distributions, the likelihood function would not necessarily be in terms of a simple residual norm.

Given its structure, *L* is amenable to a hierarchical maximization with respect to the unknown parameters. We define a "reduced" likelihood function which, for each fixed hypocenter, is minimum with respect to *t* and σ (subject to prior constraints on σ):

$$\tilde{L}(\mathbf{x};\mathbf{d}) = \max_{t,\sigma} L(\mathrm{x}, t, \sigma; \mathrm{d}). \tag{7}$$

For general $p \ge 1$, this maximization over *t* and σ can be performed with a combination of analytical and root-finding techniques. The location problem reduces to maximization of $\tilde{L}$ with respect to **x**.

Grid Search

Our grid search algorithm computes the reduced likelihood function, $\tilde{L}$ in equation (7), at each point in a 3-D grid of hypocenters. Following previous workers, the hypocenter grid is constructed dynamically through a process of successive refinement. Our procedure for grid refinement resembles that of the "neighborhood" search algorithm developed by Sambridge (1999). If the search is not restricted to a specified region, the first grid covers the entire globe and 0 to 700 km in depth at a coarse spacing: 100 km in depth, 9° in latitude, and 9° in longitude near the equator and increasing at higher latitudes. On each pass of grid refinement, nodes are added as neighbors of a subset of grid points comprising the "best" (largest $\tilde{L}$) points tested thus far. Neighbors are placed at one-third the grid-spacing of the previous pass. The size of the grid subset chosen for refinement is reduced on each pass. The search ends when the grid spacing is less than 0.3 km.

Non-Elliptical Confidence Regions

In conventional event location algorithms, confidence regions on the hypocenter, epicenter and depth of an event are computed under the assumptions that the data errors are Gaussian ($p = 2$) and that the travel-time functions, $T_i(\mathbf{x})$, are well approximated as locally linear near $\mathbf{x} = \mathbf{x}_{\mathrm{ml}}$. These assumptions lead to hypocenter and epicenter confidence regions that are elliptical in shape. The size of the confidence regions, for a given confidence level, is scaled by a critical value of the F distribution for an appropriate number of degrees of freedom, as determined by a prior assumption about the data variance, σ^2. This approach is developed by Flinn (1965), Evernden (1969) and Jordan and Sverdrup (1981) under differing assumptions about σ^2 (unknown, known and partially known, respectively).

We have generalized this approach to avoid the linearity approximation and to allow for non-Gaussian data errors and arbitrary parameter constraints. As in the conventional approach, we define a confidence region in terms of a test statistic, τ, which is a function of the data and parameters being tested. For a hypocenter confidence region, we write the statistic as $\tau(\mathbf{d}, \mathbf{x})$. The confidence region, at confidence level β (e.g., $\beta =$ 90%), comprises those values of **x** that satisfy the inequality

$$F\left[\tau(\mathbf{d},\mathbf{x})\right] \le \beta \tag{8}$$

where **d** is the observed data vector, and $F[\ ]$ denotes the cumulative distribution function (c.d.f.) of a random variable. Following a well known statistical approach, we define the test statistic as the logarithm of a likelihood ratio:

$$\tau(\mathbf{d},\mathbf{x}) = \log \tilde{L}(\mathbf{x}_{\mathrm{m1}};\mathbf{d}) - \log \tilde{L}(\mathbf{x};\mathbf{d}) = \log\left[\frac{\max_{\mathbf{x},t,\sigma} L(\mathbf{x},t,\sigma;\mathbf{d})}{\max_{t,\sigma} L(\mathbf{x},t,\sigma,\mathbf{d})}\right] \tag{9}$$

That is, for given **x**, τ compares the difference between the maximum likelihood (achieved by $\mathbf{x}_{\mathrm{ml}}$) and the likelihood achieved by **x**. Since the inequality (8) rejects large values of τ, confidence regions will exclude hypocenters that achieve relatively small values of likelihood, i.e., poor fits to the data. We point out that under the Gaussian, linear assumption, the likelihood ratio statistic is equivalent to the variance ratio on which elliptical confidence regions are based.

The statistic for a 2-D confidence region on the event epicenter, (θ,ϕ), is defined by

$$\tau(\mathbf{d},\theta,\phi) = \log\tilde{L}(\mathbf{x}_{\mathrm{m1}};\mathbf{d}) - \log \max_{z} \tilde{L}(\theta,\phi,z;\mathbf{d}) \tag{10}$$

and for a confidence interval on focal depth we use

$$\tau(\mathbf{d},z) = \log\tilde{L}(\mathbf{x}_{\mathrm{m1}};\mathbf{d}) - \log \max_{\theta,\phi} \tilde{L}(\theta,\phi,z;\mathbf{d}). \tag{11}$$

Confidence regions using these log-likelihood statistics could still be defined via the inequality of equation (8), except this inequality presumes that the distribution (c.d.f.) of τ does not depend on the true values of parameters that are not being tested. To address this, we assume the main dependence is on focal depth and σ, and rewrite the c.d.f. of τ as $F[\tau,z,\sigma]$. We generalize the inequality of equation (8) to use the c.d.f. of τ that is minimum with respect to the untested parameters. Thus, the hypocentral confidence region is given by

$$\min_{\sigma} F\left[\tau(\mathbf{d},\mathbf{x});z,\sigma\right] \le \beta. \tag{12}$$

The epicentral confidence region is

$$\min_{\sigma,z} F\left[\tau(\mathbf{d},\theta,\phi);z,\sigma\right] \le \beta \tag{13}$$

and the focal depth confidence interval is

$$\min_{\sigma} F\left[\tau(\mathbf{d},z);z,\sigma\right] \le \beta \tag{14}$$

With these definitions, a confidence region will include the true value of the tested parameters *at least* 100β percent of the time.

Confidence Regions Via Monte Carlo Sampling

Without assumptions like linearity of T_i, it is not possible to derive an analytic expression for the c.d.f. of τ, which is needed to compute confidence regions. However, we can approximate the c.d.f. using Monte Carlo simulation. We outline the technique for hypocentral confidence regions. The basic idea is to estimate the c.d.f. of the test statistic τ by simulation, i.e. computing τ for many randomly generated samples of the error vector. We generate each error, e_i^{mc}, using a pseudo-random number generator in accordance with the assumed error distribution [eqs. (2)–(3)] for some given "true" σ. Then, for given true hypocentral parameters, **x** and t, synthetic data are calculated as

$$d_i^{\mathrm{mc}} = t + T_i(\mathbf{x}) + e_i^{\mathrm{mc}}. \tag{15}$$

We apply our grid search algorithm to these data to obtain the maximum-likelihood hypocenter, $\mathbf{x}_{\mathrm{m1}}^{\mathrm{mc}}$. Plugging this into the formula for τ,

$$\tau(\mathbf{d}^{\mathrm{mc}},\mathbf{x}) = \log\tilde{L}(\mathbf{x}_{\mathrm{m1}}^{\mathrm{mc}};\mathbf{d}^{\mathrm{mc}}) - \log\tilde{L}(\mathbf{x};\mathbf{d}^{\mathrm{mc}}), \tag{16}$$

we obtain one sample from $F[\tau;z,\sigma]$. We compare this sample to the observed value of the statistic, $\tau(\mathbf{d},\mathbf{x})$, obtained from the real data. We count a rejection of **x** if

$$\tau(\mathbf{d}^{\mathrm{mc}},\mathbf{x}) < \tau(\mathbf{d},\mathbf{x}) \tag{17}$$

The proportion of rejections after many Monte Carlo trials yields an estimate of $F[\tau(\mathbf{d},\mathbf{x});z,\sigma]$. Performing this simulation for multiple values of σ and then minimizing amongst them gives the *lowest* confidence level such that the confidence region includes **x**.

The process for depth confidence intervals and epicenter confidence regions proceeds in the same manner, except that in the latter case the simulation is performed for multiple values of true depth as well as σ, and the confidence level is minimized over both.

Examples From the Racha and Adana Earthquake Sequences

Figure 1 shows confidence regions computed for an event from the 1991 Racha, Georgia, earthquake sequence, studied by Myers and Schultz (2000). The data set comprises P wave arrival times at six regional stations, obtained from the International Seismological Centre (ISC) with two stations re-picked by Lawrence Livermore National Laboratory (LLNL). We computed confidence regions with our Monte Carlo/grid search algorithm two ways. First, we assumed the picking errors are from a Gaussian distribution, with the standard deviation constrained between 1.0 and 2.0 seconds for the ISC picks and between 0.5 and 1.0 seconds for LLNL picks. Second, we assumed the errors were from an exponential distribution (p = 1), with the same constraints applied to the standard errors. In both cases, we used the travel-time tables for the IASPI91 Earth model.

The results in Figure 1 illustrate the effect of nonlinearity on the confidence regions of sparsely recorded events. Even in the Gaussian case (top), we see that the epicenter and hypocenter confidence regions depart significantly from ellipses. This is due largely to the fact that the event depth is poorly constrained by first arrivals from only six stations covering a limited distance range (6° to 22°). Travel time does not behave as a linear function over the wide range of event depths that is consistent with the data.

Comparing the top and bottom portions of Figure 1, we see that the confidence regions for Gaussian and exponential error distributions are similar, but not identical, in shape. More noticeable is the fact that the exponential ones are bigger at high levels of confidence, above 90%. This is consistent with the larger tails of the exponential distribution. However, only confidence regions at very high confidence levels, particularly in the Gaussian case, include the local network location. This was generally the case for 18 Racha events we analyzed, all of which had six or fewer data. For the 14 of these events whose epicenters were reasonably constrained, the locations were consistently mislocated by roughly 40 km north-northwest of the true location. These results are consistent with those of Myers and Schultz (2000), who showed that the mislocations are due to the need for travel-time corrections as large as 3 seconds at some stations.

As further examples, Figure 2 shows confidence regions determined with Gaussian and exponential error assumptions for the 27 June 1998 M=6.2 Adana earthquake, and Figure 3 shows the same for its largest aftershock on 4 July 1998. The data used in these examples are from the Reviewed Event Bulletin (REB) of the International Data Centre. Only first arrival P times were used in our calculations, which numbered 24 for the mainshock and 20 for the aftershock. For both the Gaussian and exponential error models, the standard error (σ) was bounded between 0.5 and 1.5 seconds.

In the case of Gaussian errors (top of Figures 2 and 3) we do not see strong non-ellipticity of the confidence regions because the confidence regions are small compared to the distances to the stations, and they are contained mainly in the upper mantle where there are no large velocity contrasts (in the IASPI91 model). Despite these factors, though, there is noticeable departure of the confidence regions from ellipses in the case of exponentially distributed errors (bottom of figures).

Once again, only confidence regions at high confidence levels cover the true locations of the Adana events, as inferred from a dense local network that surrounded the events (Aktar et al, 2000). The fact that the mislocation is similar (west and deep) for the two events suggests it is not due to picking errors that were anomalously large compared to our assumed picking accuracy, which was itself rather large (standard error of up to 1.5 seconds).

Modeling Errors

In the examples above, reasonable assumptions about picking errors do not yield valid conclusions about the uncertainty in event locations. The confidence regions do not include the true event locations except at high confidence levels, and the mislocation is similar for different events in the same region, suggesting a repeatable source of error. Errors in travel-time models frequently exceed picking errors and, when they cannot be corrected, must be accounted for in the uncertainty analysis.

A simple, and commonly used, way to do this is to inflate the assumed variance of the data errors, attempting thus to define the probability distribution of the sum of picking and modeling errors [$c_i + e_i$ in equation (1)]. This would be appropriate if modeling errors were independent between stations and seismic phases. Another mechanism is to modify the shape, as well as the width, of the error distribution, e.g., manipulating p as we did in the examples. However, to the extent that modeling errors are correlated between stations and phases, the confidence regions that result might still not be indicative of the true location error. Ultimately, a statistical analysis of actual picking and modeling errors is needed to derive an appropriate error model.

We are currently pursuing a formal approach to the problem by attempting to link the effects of modeling errors in the single event location problem to empirical calibration methods. Such methods fit travel-time residuals observed from many events with parameterized corrections. An analysis of the errors in the correction estimates provides the statistical model of modeling errors that we need.

For example, many approaches to calibration (e.g., Dewey, 1971; Jordan and Sverdrup, 1981; Pavlis and Booker, 1983) assume that travel-time corrections are static at stations (i.e. independent of event location) and then solve the problem of jointly determining the locations of multiple events and the station corrections. The problem can be posed as

$$d_{ij} = t_j + T_i(\mathbf{x}_j) + c_i + e_{ij}, \quad i = 1,....,n;\ j = 1,....,m \tag{18}$$

for m events with origin parameters $(\mathbf{x}_j, t_j),\ j = 1,....,m$. (We have not denoted it, but we do not assume there are data for all mn possible (i,j) pairs.) Applying our maximum-likelihood formulation to this problem, we can define a solution as maximization of the likelihood function given by

$$-\log L(\mathbf{x}_1, t_1, ..., \mathbf{x}_m, t_m, \mathbf{c}; \mathbf{d}) =$$

$$K_1 + K_2 \sum_{ij} \left| d_{ij} - t_j - T_i(\mathbf{x}_j) - c_i \right|^p / (\nu_{ij})^p \tag{19}$$

where $\mathbf{c} = (c_1,\ldots,\boldsymbol{c}_n)$, $\mathbf{d}$ denotes the vector of data from all events, and K_1 and K_2 are constants. A complete solution of this problem yields a probability distribution of an estimator for $\mathbf{c}$, which could then be used as a modeling error distribution in locating a new event. An even more rigorous approach would be to include each new event in the multiple-event analysis and infer its location uncertainty directly, accounting for the trade-offs amongst event locations and travel-time corrections.

The assumption of source-independent station corrections restricts a calibration analysis of this type to events that are in a tight cluster. To address calibration with events distributed over a wide region, it is necessary to consider the spatial dependence of travel-time corrections. A geo-statistical approach to this problem was formulated by Schultz et al (1998), who applied a kriging method to interpolate observed travel-time residuals between events. We are investigating an analysis of modeling errors using this approach. In this analysis, a travel-time correction is a *path*-dependent term, c_{ij}. A prior error model for the c_{ij} is specified by considering them to be samples of a random field. We are formulating this approach with a universal parameterization of corrections for all stations. A simple example, assuming only P wave data so as to avoid new notation, is to define a single random field, $(\mathbf{x})$, and let

$$c_{ij} = a(\mathbf{y}_i) + a(\mathbf{x}_j) \tag{20}$$

where $\mathbf{y}_i$ is the location of the ith station. The uncertainty analysis for an event location now falls out of the joint inversion problem of multiple-event location and kriging.

Approaches such as this provide a rigorous framework for addressing the uncertainty in seismic event locations and the effects of both observational and modeling errors. However, they do not necessarily lead to practical algorithms for accomplishing the analysis. We are investigating the feasibility of applying our grid search and Monte Carlo techniques to the problem, and seeking approximations and shortcuts that can accomplish the basic goals of the approach in a practical way.

CONCLUSIONS AND RECOMMENDATIONS

We have developed a general theoretical and computational framework for characterizing the uncertainty in seismic event locations. Applications to date show that, for sparsely recorded events or poor station distribution, the elliptical confidence regions resulting from a linear, Gaussian analysis do not adequately characterize this uncertainty. The effects appear to be significant when the true confidence region is too large compared to event-station distances, or encompasses significant variations in the Earth's velocity. An example of the latter situation is when the data allow focal depths ranging through the crust and upper mantle, which is a common occurrence when only first arrivals are used. The use of non-Gaussian error distributions can also lead to non-elliptical confidence regions.

As part of our uncertainty analysis, we are attempting to include a realistic model of the errors in the travel-time tables used in locating an event. We are pursuing an approach that links the error model used in single-event location to the results of calibration analyses performed with multiple-event data. To test our ideas, we are preparing a large database of events in Turkey that are recorded by local and national networks spanning the country, many of which are recorded by regional and teleseismic stations. These data will enable us to study the size and spatial dependence of travel-time residuals, and also provide accurate locations for many small events so we can validate the confidence regions we derive from sparse regional networks.

REFERENCES

Aktar, M., M. Ergin, S. Özalaybey, C. Tapirdamaz, A. Yörük and F. Bicmen (2000). A Lower-Crustal Event in the Northeastern Mediterranean: The 1998 Adana Earthquake (M_w=6.2) and Its Aftershocks, *Geophys. Res. Letters, 27,* 2361-2364.

Billings, S. D., M. S. Sambridge and B. L. N. Kennett (1994). Errors In Hypocenter Location: Picking, Model and Magnitude Dependence, *Bull. Seism. Soc. Am., 84,* 1978-1990.

Dewey, J. W. (1971). Seismicity Studies with the Method of Joint Hypocenter Determination, *Ph.D. Thesis*, University of California, Berkeley.

Evernden, J. F. (1969). Precision of Epicenters Obtained By Small Numbers of World-Wide Stations, *Bull. Seism. Soc. Am., 59,* 1365-1398.

Flinn, E. A. (1965). Confidence Regions and Error Determinations for Seismic Event Location, *Rev. Geophys., 3,* 157-185.

Jeffreys, H. (1932). An Alternative to the Rejection of Observations, *Mon. Not. R. Astr. Soc, Geophys. Suppl. 2,* 78-87.

Jordan, T. H. and K. A. Sverdrup (1981). Teleseismic Location Techniques and Their Application to Earthquake Clusters in the South-Central Pacific, *Bull. Seism. Soc. Am., 71,* 1105-1130.

Myers, S. C., and C. A. Schultz (2000). Improving Sparse Network Seismic Locations with Bayesian Kriging and Teleseismically Constrained Calibration Events, *Bull. Seism. Soc. Am., 90,* 199-211.

Pavlis, G. L., and J. R. Booker (1983). Progressive Multiple Event Location (PMEL), *Bull. Seism. Soc. Am., 73,* 1753-1777.

Sambridge, M. (1999). Geophysical Inversion with a Neighbourhood Algorithm - 1. Searching a Parameter Space, *Geophys. J. Int., 138,* 479-494.

Schultz, C. A., S. C. Myers, J. Hipp and C. J. Young (1998). Nonstationary Bayesian Kriging: A Predictive Technique to Generate Spatial Corrections for Seismic Detection, Location, and Identification, *Bull. Seism. Soc. Am., 88,* 1275-1288.

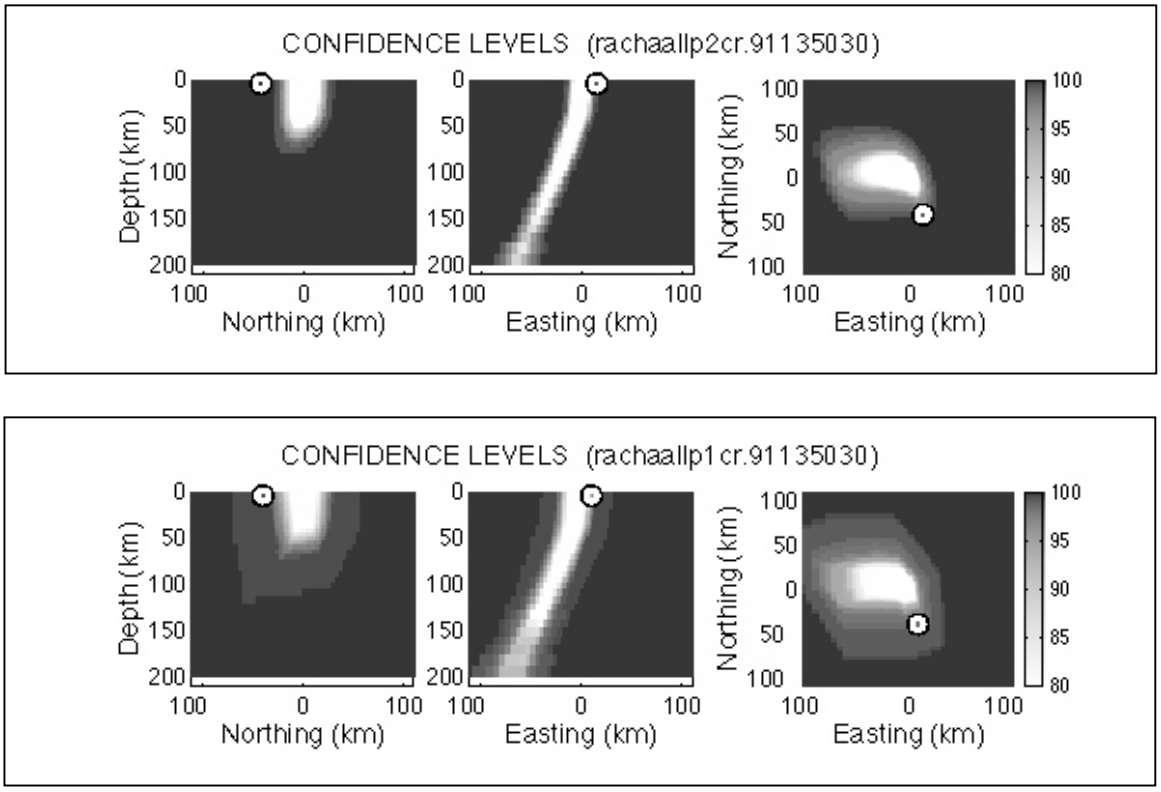

Figure 1: Confidence level vs. location for an event from the 1991 Racha earthquake sequence (ID 91135030). The top panels are based on the assumption of Gaussian picking errors (p=2). The bottom panels assume the errors are from an exponential distribution (p =1). *Left and center:* Cross-sections of confidence level vs. hypocenter taken through the maximum-likelihood location. *Right:* Confidence level vs. epicenter. Each contour of constant confidence level is the boundary of the 3-D hypocenter (left and center) or epicenter (right) confidence region at that level. Note that confidence levels below 80% are all displayed with white. The circles mark the local network location for the event. The maximum-likelihood epicenter is at zero northing and zero easting.

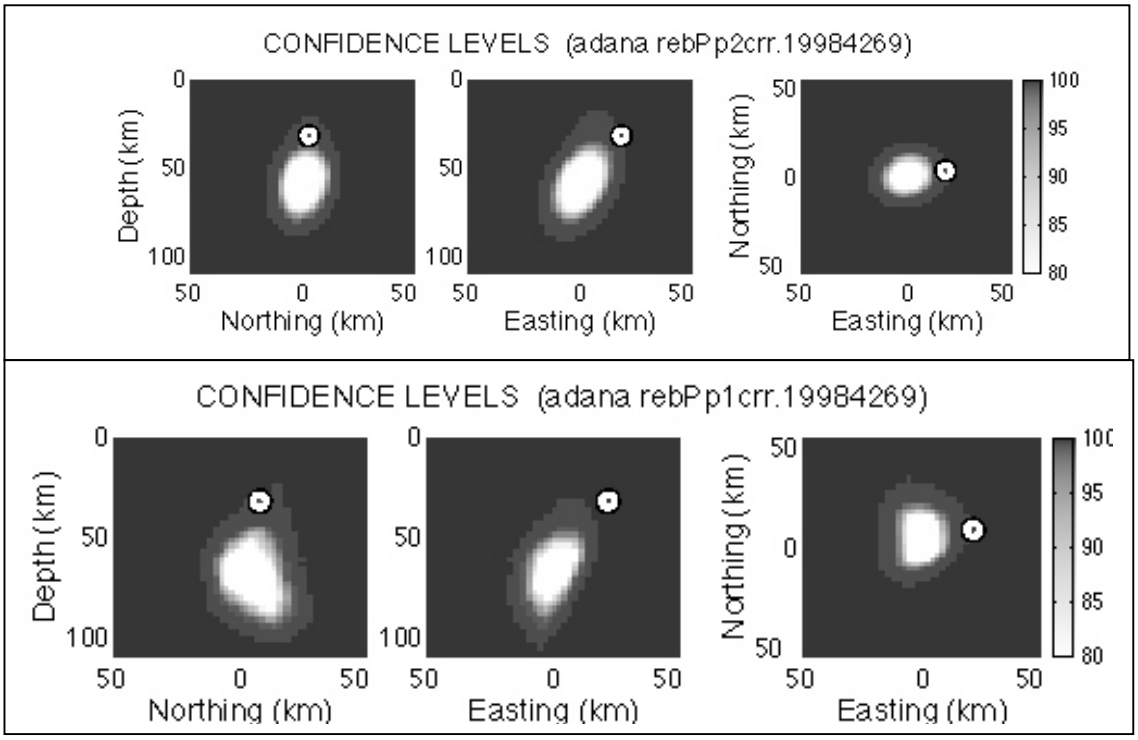

Figure 2: Confidence level vs. location for the 27 June 1998 Adana earthquake, determined with a Gaussian (top) and exponential (bottom) error model. The panels are defined as in Figure 1. The circles mark the local network location for the event.

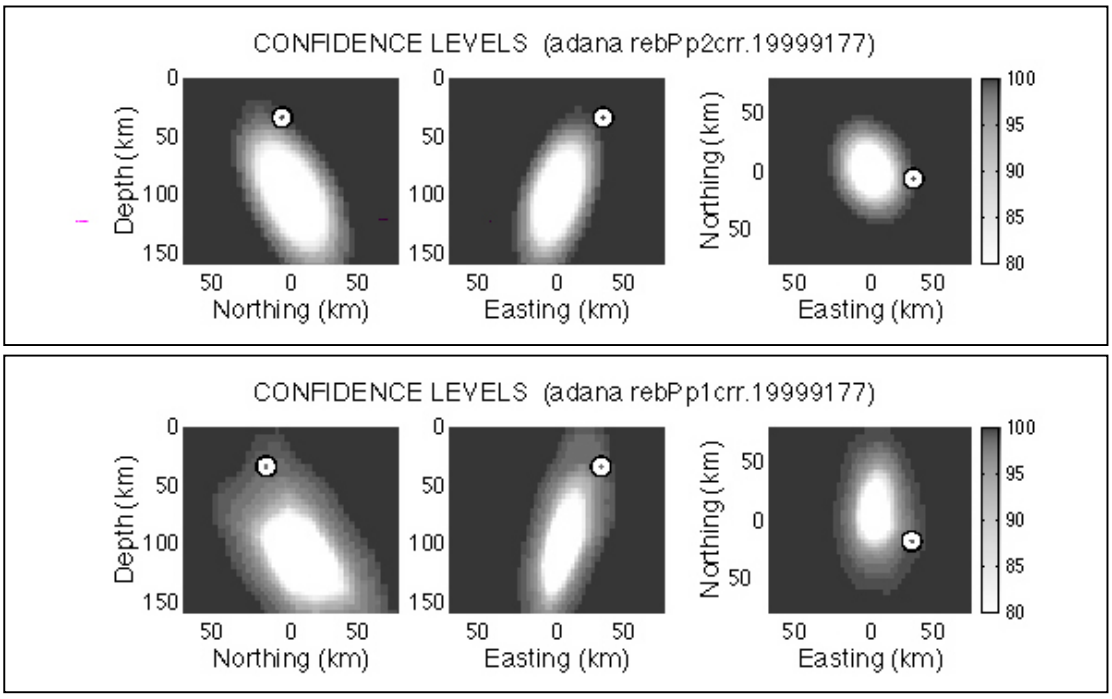

Figure 3: Confidence level vs. location for the 4 July 1998 aftershock of the Adana earthquake, shown in the same format as Figure 2.